Int. J. Solids Structures, 1975, vol. 11, pp. 53–73. Pergamon Press, Printed in Gt. Britain.

ON THE BEHAVIOR OF STRESS WAVES IN COMPOSITE MATERIALS—I. A UNIVERSAL SET OF BOUNDARY CONDITIONS†

D. S. DRUMHELLER and F. R. NORWOOD

Members of Technical Staff Sandia Laboratories, Albuquerque, New Mexico 87115, U.S.A.

(*Received* 13 *December* 1973)

Abstract—In recent years experiments on uniaxially reinforced composites have revealed anomalous behavior in the stress-wave propagation characteristics of these materials. Whenever the exposed ends of both composite constituents were subjected to moderate pressures of a few kilobars the number of stable propagating waves generated within the composite exceeded by one the number of waves calculated through conventional composite models. This effect greatly increased the wave dispersion and rise-time in the experimentally observed stress wave.

The key to the origin of this phenomenon is quite elementary. The composite debonds internally. When the bond between the reinforcing and matrix fails, the composite attains an additional degree of freedom which results in an additional stable propagating wave. Since conventional composite models do not allow for this debonding, they cannot account for the resulting wave. However, as was shown in an earlier paper, direct application of the theory of elasticity to this problem results in wave velocities and mode shapes for all of the waves.

The solution to the total problem, including the determination of the various wave amplitudes, was previously hampered by an insufficient set of boundary conditions. The usual procedure was to impose continuity of stress and displacement at the boundary between the composite and the adjoining homogeneous material where the volumetric averages of stress and displacement were used for the composite. While these conditions are necessary and sufficient for the bonded composite problem, they are insufficient for the debonded composite problem. The additional degree of freedom in the debonded problem makes the use of an additional boundary condition necessary. This additional boundary condition is the subject of this paper.

INTRODUCTION

In studying the behavior of composite materials, one encounters many problems not found in analyzing homogeneous materials. One of these problems is the determination of appropriate boundary conditions at the interface of a composite and a homogeneous material. In the case of two homogeneous materials, the requisite boundary conditions are continuity of stresses and displacements along the interface. In the case of composite materials, a complete description of the boundary conditions yields a system of equations which is formidable, if not impossible, to solve. This leads to the consideration of alternate descriptions that make the solution to a boundary value problem more tractable. As an example, suppose that one is dealing with the geometry in which the region $x > 0$ is occupied by a composite, while the region $x < 0$ is occupied by a homogeneous elastic material. It is obvious that very complex stress and displacement fields exist near $x = 0$. However, as the distance from the interface increases, these fields assume a much simpler form[1, 2]. Consequently, unless detailed information is required near the interface, the complex boundary conditions associated with the exact solution can be replaced by simpler conditions. These simpler boundary conditions

† This work was supported by the United States Atomic Energy Commission.

should provide the necessary coupling between the stable far-field solutions in the homogeneous material and in the composite, and, in particular, for dynamical problems the simpler boundary conditions must relate the shear and dilatational waves in the homogeneous material to the stable propagating waves in the composite.†

It has been shown[1] that these stable modes of propagation can be studied by first evaluating the response of the composite to time–harmonic waves, and then finding the limit as the frequency approaches zero. The time–harmonic response consists of an infinite variety of modes, with only a finite number remaining in the limit of zero frequency representing the static solution. These remaining modes are the stable propagation modes of the composite which determine the average far-field response of the composite. Since the effect of geometric dispersion caused by the heterogeneity of the composite is only a perturbation to the stable modes, the gross or average dynamical response of the composite may be evaluated by considering the static behavior. While the boundary conditions to be deduced are not limited to this type of approach, this method will be used to facilitate the analysis.

For a laminated composite in which the constituents are fully bonded, Sve[5] has shown that the stable propagation modes are analogous to those in a homogeneous medium; i.e. the composite has two stable propagation modes: a longitudinal and a shear mode. More recent work[6] has shown that, when the constituents undergo internal debonding, the laminated composite can support three stable modes of stress wave propagation. These three modes are a shear mode, a longitudinal mode in which adjacent plates slide in opposite directions, and a longitudinal mode with adjacent plates moving in the same direction.

Comparison to actual flyer-plate experiments has shown that the assumption of a fully bonded composite leads to agreement with these experiments only for low stress levels or when the load is applied perpendicular to the interface planes; and, otherwise, it leads to gross discrepancies. One of these discrepancies is the appearance of an additional stable propagation mode in flyer-plate experiments in which the composite was subjected to moderate pressures of a few kilobars[6]. The assumption of internal debonding used in[6] provided an extra degree of freedom allowing for an additional stable wave to be generated in the composite. The computed wave speed for this wave agreed fairly well with the experiments; however, the solution of transient problems, including the determination of the various wave amplitudes and profiles, was hampered by an insufficient set of boundary conditions. To correct this deficiency, attention will be focused in the rest of this paper on establishing a set of boundary conditions for a properly posed problem. These boundary conditions will apply equally well to laminated or fiber-reinforced composites. For definiteness in the rest of this work, the geometry of Fig. 1 will be considered, and it will be shown that these boundary conditions link the two waves in the homogeneous medium to either two or three waves in the composite material.

Finally, for clarity it seems appropriate to provide one additional illustration of the underlying problem. In Fig. 1, assume that $\theta = 0$ and that the plates in the composite are debonded. Suppose that initially a longitudinal stress wave is propagating through the homogeneous material in the positive x direction. When this wave interacts with the composite boundary, it generates a reflected longitudinal wave and two transmitted longitudinal waves. By the assumptions that $\theta = 0$ and that the plates are debonded, it follows that no shear modes are excited in either material. The solution of this boundary value

† It is important to note that these arguments are in accordance with the static Saint-Venant's principle [3, p. 33], and with the dynamic Saint-Venant's principle postulated by Jones and Norwood[4, p. 723].

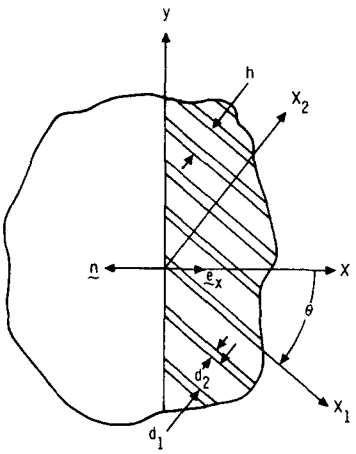

Fig. 1. The wave propagation and the material coordinate systems.

problem requires a knowledge of the propagation speeds and deformation patterns for each wave. As shown in [5], without knowledge of the boundary conditions, the speeds can be determined exactly, and the deformation patterns or mode shapes for each wave can be determined to within an arbitrary constant. For the evaluation of each arbitrary constant, one must apply the boundary conditions. In the present case, to complete the solution, it is necessary to apply three boundary conditions to solve for the three heretofore arbitrary amplitudes associated with the reflected and transmitted waves. The question that arises is: What three conditions must be imposed at $x = 0$ such that the resulting boundary value problem remains tractable? In answering this question the following two conditions appear to be a logical and obvious answer. First, the average x displacement in the composite must equal the x displacement in the homogeneous material. Second, this must also hold for the normal stress at the boundary. To complete the solution, another boundary condition must be specified.

COORDINATE SYSTEMS AND NOTATION

To simplify the development, two coordinate systems are defined as follows. The first is the x_1–x_2 material coordinate system, shown in Fig. 1, which is selected such that the x_1 axis coincides with the reinforcing direction. The second is the x–y propagation coordinate system which is oriented such that the x direction coincides with the direction of propagation of all incident, reflected, and transmitted waves. In this work, the direction of propagation is selected normal to the composite–homogeneous material interface; other directions can be treated by an obvious extension of the present work.

As in [5, 6], information about mode shapes of the various stable waves within the composite is given in terms of the material coordinates x_1–x_2. The stresses and displacements in this coordinate system are denoted by ${}_m\sigma_{ij}{}^{(k)}$ and ${}_mu_i{}^{(k)}$, where the presubscript denotes the propagation mode, the superscript denotes the composite constituent, either reinforcing or matrix, and the subscripts indicate the respective tensor and vector components. In the wave propagation system x–y, four quantities are required. They are the normal stress in the x direction $\sigma_i{}^m$, the shear stress $\tau_i{}^m$, the displacement in the x direction $u_i{}^m$, and the displacement in the y direction $v_i{}^m$. In this system, the subscript denotes the composite

constituent and the superscript denotes the propagation mode, and the component is already indicated by the symbol σ, τ, u, or v. The presubscript and superscript m which identifies the mode number will be omitted in some cases to indicate that the expression represents the summed effect of all possible modes. In the homogeneous material ($x < 0$), the normal stress in the x direction, the shear stress in the x–y system, and the displacements in the x and y directions are given by σ, τ, U and V, respectively.

Within the composite, the quantities in the propagation system are related to those in the material system through the equations

$$\begin{aligned} u_i^m &= {}_m u_1^{(i)} \cos\theta + {}_m u_2^{(i)} \sin\theta \\ v_i^m &= -{}_m u_1^{(i)} \sin\theta + {}_m u_2^{(i)} \cos\theta \\ \sigma_i^m &= {}_m\sigma_{11}^{(i)} \cos^2\theta + {}_m\sigma_{22}^{(i)} \sin^2\theta + 2{}_m\sigma_{12}^{(i)} \sin\theta\cos\theta \\ \tau_i^m &= ({}_m\sigma_{22}^{(i)} - {}_m\sigma_{11}^{(i)})\sin\theta\cos\theta + {}_m\sigma_{12}^{(i)}(\cos^2\theta - \sin^2\theta). \end{aligned} \tag{1}$$

THE BOUNDARY CONDITIONS

Consider the general case in which $\theta \neq 0$ (Fig. 1). If internal debonding occurs, then a stress wave incident on the interface $x = 0$ creates five new waves. These waves are a longitudinal wave and a shear wave in the homogeneous material occupying the region $x < 0$, and two quasi-longitudinal waves and a quasi-shear wave in the composite. If the composite constituents are bonded, then there is one less quasi-longitudinal wave in the composite. Therefore, if the composite is debonded (bonded), then five (four) independent boundary conditions must be supplied to solve for the five (four) amplitudes associated with the reflected and transmitted waves.

For the case when the composite constituents with thickness d_i are perfectly bonded and there is perfect contact at $x = 0$, then, in terms of the influence ratios η_i defined by

$$\eta_i = d_i/(d_1 + d_2), \qquad (i = 1, 2), \tag{2}$$

the conditions of continuity of average displacements and stresses can be satisfied by specifying the following four conditions†

$$\sigma = \eta_1\sigma_1 + \eta_2\sigma_2, \tag{3}$$

$$\tau = \eta_1\tau_1 + \eta_2\tau_2, \tag{4}$$

$$U = \eta_1 u_1 + \eta_2 u_2, \tag{5}$$

$$V = \eta_1 v_1 + \eta_2 v_2. \tag{6}$$

The expressions on the right side of these equations are simply the area averages of the appropriate quantities.

For the case when the composite constituents are bonded, but the homogeneous and composite materials are allowed to slide relative to each other, the appropriate boundary conditions are

$$\sigma = \eta_1\sigma_1 + \eta_2\sigma_2, \tag{7}$$

$$\tau = 0, \tag{8}$$

$$0 = \eta_1\tau_1 + \eta_2\tau_2, \tag{9}$$

$$U = \eta_1 u_1 + \eta_2 u_2. \tag{10}$$

† By the deletion of the mode superscript, then $\sigma_i = \sigma_i^1 + \sigma_i^2$.

If either set of boundary conditions are combined with the mode shape results, obtained from the field equations for each region, the amplitudes of the four waves can be evaluated.

However, if internal debonding is allowed, five stable waves will exist and an additional boundary condition will be required. The form of this boundary condition for laminated composites will be deduced by considering the nature of the interface effect depicted in Fig. 2. As shown in the figure, when the materials are compressed, the originally planar interface is not only translated, but it is also warped. With the present assumption of debonding, this warping results in the sliding of one constituent relative to the other in a periodic fashion along the interface. However, unlike the corresponding development in the bonded composite where this effect remains localized at the boundary, this effect is transmitted throughout the interior of the debonded composite and must be considered in the total solution to the problem. In writing the appropriate boundary condition to represent this warping effect, three physical quantities must be interrelated. These physical quantities are as follows: the difference between the constituent stress and the average interface stress which produces the warping, the difference between the constituent displacement and the average interface displacement which indicates the magnitude of the warping, and a stiffness factor representing the resistance of the interface to warp. It will be shown that this stiffness factor is highly dependent on the elastic properties of the homogeneous material.

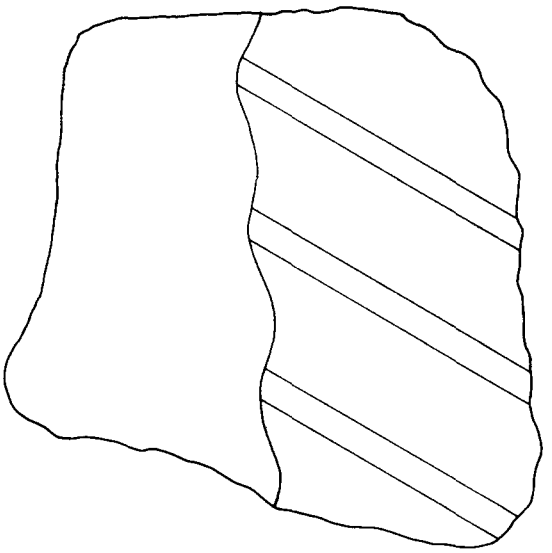

Fig. 2. Illustration of the warping effect at the composite boundary.

To define the stiffness factor, let us consider corresponding differences in x–y coordinates in constituent 1 of the composite under static conditions. The difference $\Delta\sigma$ between the normal stress in constituent 1 and the average normal stress in the x direction is

$$\begin{aligned}\Delta\sigma &= \sigma_1 - (\eta_1\sigma_1 + \eta_2\sigma_2)\\ &= \eta_2(\sigma_1 - \sigma_2).\end{aligned} \tag{11}$$

Likewise, the difference Δu between the x displacement in constituent 1 and the average x displacement is

$$\Delta u = \eta_2(u_1 - u_2). \tag{12}$$

The stiffness factor, for the warping at the interface, is defined as the ratio $\Delta\sigma/\Delta u$. This leads to

$$W = \frac{\sigma_1 - \sigma_2}{u_1 - u_2}. \tag{13}$$

The corresponding analysis for constituent 2 also results in equation (13). Consequently, equation (13) is valid at all points along the composite boundary. One now defines

$$\begin{aligned} \mathbf{n} &= \text{the composite unit outward normal vector} \\ \mathbf{e}_x &= \text{the unit vector in the } x \text{ direction,} \end{aligned} \tag{14}$$

and introduces the dot product $(-\mathbf{n} \cdot \mathbf{e}_x)$ into equation (13) to make it applicable when the position of the composite and the homogeneous material are interchanged. Thus, the final form of the required fifth boundary condition is

$$W = (-\mathbf{n} \cdot \mathbf{e}_x) \frac{\sigma_1 - \sigma_2}{u_1 - u_2}. \tag{15}$$

It now remains to evaluate the stiffness factor W. In general, this factor depends on both the warping stiffness of the composite and the homogeneous material; however, for a debonded composite, the warping stiffness of the composite is zero. The warping stiffness also depends on the bond at the interface. By allowing frictionless sliding at this boundary, only the effects of normal stress and x displacement will be transmitted across the boundary.† Consequently, this constant depends on the angle θ, the dimension $h = d_1 + d_2$, the elastic properties of the homogeneous material, and the type of stress boundary condition assumed at $x = 0$. When this boundary condition allows for frictionless sliding, W can be evaluated by considering a self-equilibrated system of line loads applied to the homogeneous medium as shown by the solid arrows in Fig. 3. One finds that

$$W = \frac{2{\cdot}414 \cos\theta}{h} \cdot \frac{G}{1 - \nu}, \tag{16}$$

where the details of the calculation have been relegated to Appendix A. In this equation G and ν are the shear modulus and the Poisson ratio, respectively, for the homogeneous medium. From preliminary calculations of stiffness factors for various interface conditions involving debonded laminated and fiber-reinforced composites, it appears that W consists of the ratio $G/(1 - \nu)$ times a geometric factor.

In applying equation (15) to a bonded composite when $\theta = 0$, one has that $u_1 = u_2$ and $\sigma_1 \neq \sigma_2$, so that equation (15) would require W to be infinite. Since in this case W also depends on the warping stiffness of the composite, and since the class of solutions for the bonded composite field equations exclude any warping, this result is to be expected. Thus, there can be no warping at the boundary and the remaining four boundary conditions are

† This fact is implicit in the definition of W via equation (15).

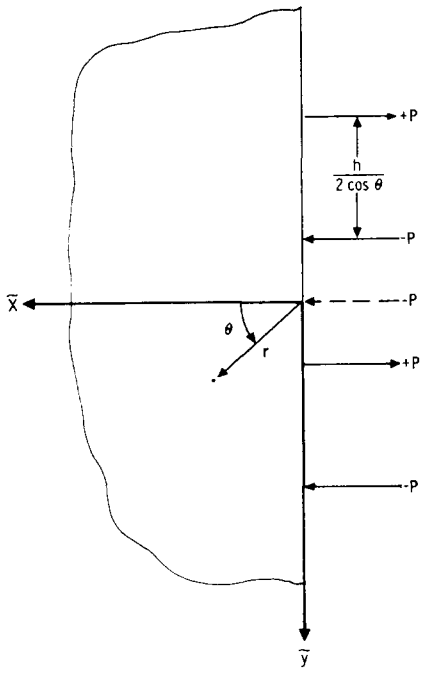

Fig. 3. Force diagram for the calculation of W.

sufficient to solve the bonded composite problem. In the case $\theta = \pi/2$, regardless of the bonding assumption, again there is no warping at the boundary and equation (15) requires that $\sigma_1 = \sigma_2$; this is a duplication of the results obtained from the field equations of the composite.

THE STATIC COMPRESSION TEST

For the first application of the boundary conditions consider the evaluation of the apparent gross compressional stiffness of the composite via the one-dimensional strain compression test depicted in Fig. 4. A laminated plate composite of length $2L$ is sandwiched between two identical buffer blocks and loaded with a static force P. In the analysis, buckling of the composite constituents is ignored. Since $\theta = 0$, only the two longitudinal modes for $m = 1, 2$ are excited in the composite. Thus, the shear mode and the boundary conditions connected with shear deformation may be ignored. The appropriate boundary conditions at $x = 0$ are

$$\begin{aligned} u_1^{\,1} + u_1^{\,2} &= 0, \\ u_2^{\,1} + u_2^{\,2} &= 0; \end{aligned} \tag{17}$$

and at $x = L$,

$$\begin{aligned} \sigma = P/A &= \eta_1(\sigma_1^{\,1} + \sigma_1^{\,2}) + \eta_2(\sigma_2^{\,1} + \sigma_2^{\,2}) \\ U &= \eta_1(u_1^{\,1} + u_1^{\,2}) + \eta_2(u_2^{\,1} + u_2^{\,2}) \\ -W &= \frac{\sigma_1^{\,1} + \sigma_1^{\,2} - \sigma_2^{\,1} - \sigma_2^{\,2}}{u_1^{\,1} + u_1^{\,2} - u_2^{\,1} - u_2^{\,2}}. \end{aligned} \tag{18}$$

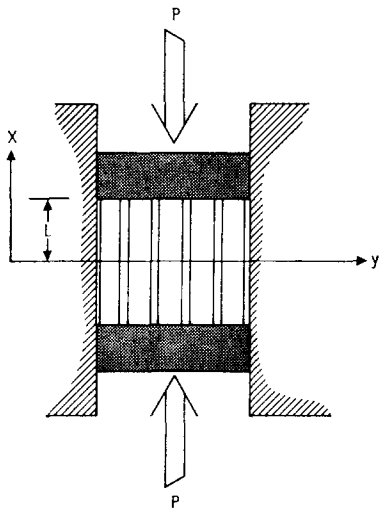

Fig. 4. Schematic of the static compression experiment.

U is the average displacement of the boundary at $x = L$, and A denotes the area over which the load is applied.

The second of equations (17) may be written as

$$u_1{}^1\left[\frac{u_2{}^1}{u_1{}^1}\right] + u_1{}^2\left[\frac{u_2{}^2}{u_1{}^2}\right] = 0, \qquad \text{at} \quad x = 0, \tag{19}$$

where the ratios in the brackets can be determined from the solution of the field equations in the composite by the procedure given in Appendix B. From (19) and the first of equations (17), it follows that

$$u_1{}^1 = u_1{}^2 = 0, \quad \text{at} \quad x = 0. \tag{20}$$

As was done in equation (19), equations (18) will now be written in terms of $u_1{}^1$, $u_1{}^2$ and mode ratios. At $x = L$,

$$\begin{gathered} \sigma = \mathfrak{E}_1 u_1{}^{1'} + \mathfrak{E}_2 u_1{}^{2'}, \\ U = \mathfrak{F}_1 u_1{}^1 + \mathfrak{F}_2 u_1{}^2, \\ \mathfrak{K}_1 u_1{}^{1'} + \mathfrak{K}_2 u_1{}^{2'} = -W[\mathfrak{G}_1 u_1{}^1 + \mathfrak{G}_2 u_1{}^2], \end{gathered} \tag{21}$$

where a prime denotes partial differentiation with respect to x and

$$\begin{aligned} \mathfrak{E}_i &= \eta_1 \frac{\sigma_1{}^i}{u_1{}^{i'}} + \eta_2 \frac{\sigma_2{}^i}{u_1{}^{i'}}, \\ \mathfrak{F}_i &= \eta_1 + \eta_2 \frac{u_2{}^i}{u_1{}^i}, \\ \mathfrak{K}_i &= \frac{\sigma_1{}^i}{u_1{}^{i'}} - \frac{\sigma_2{}^i}{u_1{}^{i'}}, \\ \mathfrak{G}_i &= 1 - \frac{u_2{}^i}{u_1{}^i}. \end{aligned} \tag{22}$$

The factors defined in (22) are stiffness and displacement coefficients which are determined from the composite field equations.

The field equations for the present case of homogeneous deformations require that the displacements be linear functions of x. Therefore, by boundary condition (20), ${u_1}^1$ must be of the form

$$ {u_1}^1 = a\sigma x, \tag{23} $$

where a is a constant to be determined. By considering the gross equilibrium of the composite, one finds that the average internal stress at any x cross-section must equal σ. This implies that the first of equations (21) holds, not only at $x = L$, but throughout the composite. Therefore it can be integrated to give

$$ \mathfrak{E}_1 {u_1}^1 + \mathfrak{E}_2 {u_1}^2 = \sigma x, \tag{24} $$

where the results of (20) have been used. The first application of the stiffness factor results when (23 and 24) are substituted into the last of equations (21) to determine the constant a. This substitution yields

$$ a = \frac{\mathfrak{K}_2 + WL\mathfrak{G}_2}{(\mathfrak{K}_2\mathfrak{E}_1 - \mathfrak{K}_1\mathfrak{E}_2) + WL(\mathfrak{E}_2\mathfrak{G}_1 - \mathfrak{E}_1\mathfrak{G}_2)}. $$

This equation represents the solution of the problem, for U can now be obtained by substituting (23 and 24) into the second of (21). Finally, the gross stiffness of the composite F is found to be

$$ F = \frac{PL}{UA} = \frac{(\mathfrak{K}_2\mathfrak{E}_1 - \mathfrak{K}_1\mathfrak{E}_2) - WL(\mathfrak{G}_1\mathfrak{E}_2 - \mathfrak{G}_2\mathfrak{E}_1)}{(\mathfrak{K}_2\mathfrak{F}_1 - \mathfrak{K}_1\mathfrak{F}_2) - WL(\mathfrak{G}_1\mathfrak{F}_2 - \mathfrak{G}_2\mathfrak{F}_1)}. \tag{25} $$

THE DYNAMIC COMPRESSION TEST

The flyer-plate experiment

The stiffness factor W will now be applied to the flyer-plate experiment. This experiment consists of striking the front surface of the composite with a flat-faced projectile traveling with velocity $\dot{U}^I$, where the dot denotes partial differentiation with respect to time. The experiment is designed such that, for the time of interest, a state of average one-dimensional strain exists in all material shown in Fig. 5. The measured quantity is the $\dot{U}$ component in the buffer material. It is assumed that the flyer-composite interface and the composite–buffer interface allow frictionless sliding. The space-time diagram for the experiment is shown in Fig. 6. At impact four waves are generated at $x = 0$; a longitudinal wave, R, in the homogeneous flyer plate, two longitudinal waves, (3 and 2), and a shear wave, (1), in the composite. In due course, the three waves propagate through the composite and interact with the homogeneous buffer material to produce nine reflected waves and three transmitted waves. By the assumption of sliding interfaces between flyer, composite, and buffer, no shear waves are generated in the flyer or buffer plate. To calculate the particle velocities produced by the transmitted waves, the interaction [0] will be considered in detail, and then the other interactions will only be outlined.

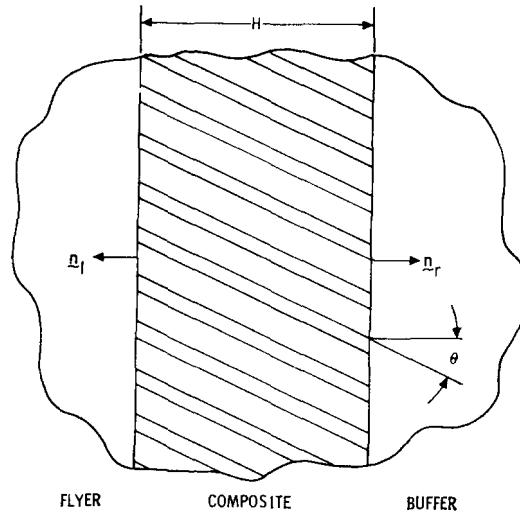

Fig. 5. Schematic of the flyer-plate experiment.

Since the flyer plate is moving with a uniform particle velocity $\dot{U}^I$, the initial flyer-plate stresses are zero. After impact, the appropriate boundary conditions at the interface $x = 0$ are given by

$$\begin{aligned} \sigma^R &= \eta_1(\sigma_1{}^1 + \sigma_1{}^2 + \sigma_1{}^3) + \eta_2(\sigma_2{}^1 + \sigma_2{}^2 + \sigma_2{}^3), \\ 0 &= \eta_1(\tau_1{}^1 + \tau_1{}^2 + \tau_1{}^3) + \eta_2(\tau_2{}^1 + \tau_2{}^2 + \tau_2{}^3), \\ \dot{U}^I + \dot{U}^R &= \eta_1(\dot{u}_1{}^1 + \dot{u}_1{}^2 + \dot{u}_1{}^3) + \eta_2(\dot{u}_2{}^1 + \dot{u}_2{}^2 + \dot{u}_2{}^3), \\ W_l &= \frac{\dot{\sigma}_1{}^1 + \dot{\sigma}_1{}^2 + \dot{\sigma}_1{}^3 - \dot{\sigma}_2{}^1 - \dot{\sigma}_2{}^2 - \dot{\sigma}_2{}^3}{\dot{u}_1{}^1 + \dot{u}_1{}^2 + \dot{u}_1{}^3 - \dot{u}_2{}^1 - \dot{u}_2{}^2 - \dot{u}_2{}^3}, \end{aligned} \tag{26}$$

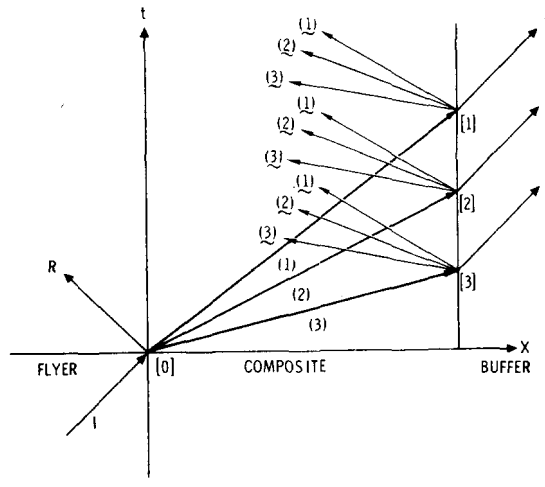

Fig. 6. Space-time diagram for the flyer-plate experiment.

where W_l is the stiffness factor associated with the flyer plate–composite interface. The last two conditions have been differentiated with respect to time for convenience. The requisite initial conditions will be specified when these relations are integrated again. In the flyer plate, stress and particle velocity are related by

$$\sigma^R = \mathscr{Z}_l \dot{U}^R, \tag{27}$$

where $\mathscr{Z}_l$ is the mechanical impedance of the flyer, the mass density times the longitudinal wave velocity.

The dynamic analog of (21 and 22) will now be written for the present problem in terms of ${\sigma_1}^1$, ${\sigma_1}^2$, and ${\sigma_1}^3$, using (27). Thus, at $x = 0$,

$$\begin{aligned} \mathscr{Z}_l \dot{U}^R &= \mathscr{C}_1 {\sigma_1}^1 + \mathscr{C}_2 {\sigma_1}^2 + \mathscr{C}_3 {\sigma_1}^3 \\ 0 &= \mathfrak{D}_1 {\sigma_1}^1 + \mathfrak{D}_2 {\sigma_1}^2 + \mathfrak{D}_3 {\sigma_1}^3 \\ \dot{U}^I + \dot{U}^R &= \mathfrak{H}_1 {\sigma_1}^1 + \mathfrak{H}_2 {\sigma_1}^2 + \mathfrak{H}_3 {\sigma_1}^3 \\ \mathscr{M}_1 \dot{\sigma}_1^{\,1} + \mathscr{M}_2 \dot{\sigma}_1^{\,2} + \mathscr{M}_3 \dot{\sigma}_1^{\,3} &= W_l(\mathscr{N}_1 {\sigma_1}^1 + \mathscr{N}_2 {\sigma_1}^2 + \mathscr{N}_3 {\sigma_1}^3). \end{aligned} \tag{28}$$

The mode ratios are given by

$$\begin{aligned} \mathscr{C}_i &= \eta_1 + \eta_2 \frac{{\sigma_2}^i}{{\sigma_1}^i} \\ \mathfrak{D}_i &= (\eta_1 {\tau_1}^i + \eta_2 {\tau_2}^i)/{\sigma_1}^i \\ \mathfrak{H}_i &= (\eta_1 \dot{u}_1^{\,i} + \eta_2 \dot{u}_2^{\,i})/{\sigma_1}^i \\ \mathscr{M}_i &= 1 - \frac{{\sigma_2}^i}{{\sigma_1}^i} \\ \mathscr{N}_i &= (\dot{u}_1^{\,i} - \dot{u}_2^{\,i})/{\sigma_1}^i. \end{aligned} \tag{29}$$

These constants are determined from the field equations of the composite.

From the first three of equations (28), one finds that

$$\begin{aligned} {\sigma_1}^2 &= \frac{\mathfrak{D}_3 \dot{U}^I + {\sigma_1}^1(S_{3l}\mathfrak{D}_1 - S_{1l}\mathfrak{D}_3)}{S_{2l}\mathfrak{D}_3 - S_{3l}\mathfrak{D}_2} \\ {\sigma_1}^3 &= \frac{\mathfrak{D}_2 \dot{U}^I + {\sigma_1}^1(S_{2l}\mathfrak{D}_1 - S_{1l}\mathfrak{D}_2)}{S_{3l}\mathfrak{D}_2 - S_{2l}\mathfrak{D}_3} \end{aligned} \tag{30}$$

where

$$S_{il} = \mathfrak{H}_i - \frac{\mathscr{C}_i}{\mathscr{Z}_l}. \tag{31}$$

Recalling that $\dot{U}^I$ is a constant, the substitution of (30 and 31) into the last of (28) yields

$$a_l \dot{\sigma}_1^{\,1} + b_l {\sigma_1}^1 = c_l \tag{32}$$

where a_l, b_l and c_l are given by

$$\begin{aligned} a_l &= (S_{2l}\mathfrak{D}_3 - S_{3l}\mathfrak{D}_2)\mathscr{M}_1 + (S_{3l}\mathfrak{D}_1 - S_{1l}\mathfrak{D}_3)\mathscr{M}_2 + (S_{1l}\mathfrak{D}_2 - S_{2l}\mathfrak{D}_1)\mathscr{M}_3 \\ b_l &= -W_l(S_{2l}\mathfrak{D}_3 - S_{3l}\mathfrak{D}_2)\mathscr{N}_1 + (S_{3l}\mathfrak{D}_1 - S_{1l}\mathfrak{D}_3)\mathscr{N}_2 + (S_{1l}\mathfrak{D}_2 - S_{2l}\mathfrak{D}_1)\mathscr{N}_3 \\ c_l &= W_l(\mathscr{N}_2\mathfrak{D}_3 - \mathscr{N}_3\mathfrak{D}_2)\dot{U}^I. \end{aligned} \tag{33}$$

By using the integrating factor $\exp(b_l t/a_l)$, one finds the solution to equation (32) to be

$$\sigma_1{}^1 = \frac{c_l}{b_l}[1 - \exp(-b_l t/a_l)] + \sigma_1{}^1(t=0)\exp(-b_l t/a_l), \tag{34}$$

where $\sigma_1{}^1(t=0)$ is the initial value of $\sigma_1{}^1$. To evaluate this quantity, the initial condition $u_1 = u_2$ at $t=0$ is applied to (26). Therefore, from (15), it follows that $\sigma_1 = \sigma_2$ at $t=0$. This also follows by integrating the last of equations (28) to yield the equivalent form of $\sigma_1 = \sigma_2$ at $t=0$ in terms of the mode ratios as

$$\mathscr{M}_1\sigma_1{}^1 + \mathscr{M}_2\sigma_1{}^2 + \mathscr{M}_3\sigma_1{}^3 = 0, \quad \text{at} \quad t=0. \tag{35}$$

Substitution of (30) in (35) gives

$$\sigma_1{}^1(t=0) = \frac{\mathscr{M}_3\mathfrak{D}_2 - \mathscr{M}_2\mathfrak{D}_3}{a_l}\dot{U}^I. \tag{36}$$

The final results of the interaction can be obtained by substituting (34) into (30). These results are now written in a uniform notation as

$$\sigma_1{}^i = \gamma_i + \delta_i \exp(-b_l t/a_l) \tag{37}$$

where the γ_i are defined by

$$\begin{aligned}
\gamma_1 &= c_l/b_l \\
\gamma_2 &= \frac{\mathfrak{D}_3\dot{U}^I + \gamma_1(S_{3l}\mathfrak{D}_1 - S_{1l}\mathfrak{D}_3)}{S_{2l}\mathfrak{D}_3 - S_{3l}\mathfrak{D}_2} \\
\gamma_3 &= \frac{\mathfrak{D}_2\dot{U}^I + \gamma_1(S_{2l}\mathfrak{D}_1 - S_{1l}\mathfrak{D}_2)}{S_{3l}\mathfrak{D}_2 - S_{2l}\mathfrak{D}_3}
\end{aligned} \tag{38}$$

and the δ_i are defined by

$$\begin{aligned}
\delta_1 &= \sigma_1{}^1(t=0) - \gamma_1 \\
\delta_2 &= \delta_1\frac{S_{3l}\mathfrak{D}_1 - S_{1l}\mathfrak{D}_3}{S_{2l}\mathfrak{D}_3 - S_{3l}\mathfrak{D}_2} \\
\delta_3 &= \delta_1\frac{S_{2l}\mathfrak{D}_1 - S_{1l}\mathfrak{D}_2}{S_{3l}\mathfrak{D}_2 - S_{2l}\mathfrak{D}_3}.
\end{aligned} \tag{39}$$

The next step in the solution is the analysis of interactions[1, 2 and 3] depicted in Fig. 6. The boundary conditions for these three interactions are similar in form, and, therefore, all three cases can be treated together. Since the interaction[0] has been treated in detail, the following need only be brief. Because the reflected waves denoted by the bold faced symbol **i** are traveling to the left, it is easy to see from (29) that

$$\begin{aligned}
&\mathscr{C}_{\mathbf{i}} = \mathscr{C}_i, \qquad \mathfrak{D}_{\mathbf{i}} = \mathfrak{D}_i, \qquad \mathscr{M}_{\mathbf{i}} = \mathscr{M}_i, \\
&\mathfrak{H}_{\mathbf{i}} = -\mathfrak{H}_i, \qquad \mathscr{N}_{\mathbf{i}} = -\mathscr{N}_i.
\end{aligned} \tag{40}$$

Suppose that the incident wave is given the label i; e.g. $i = 1$ for case [1]. Then the boundary conditions at $x = H$ for cases [1, 2 and 3] may be written as

$$\begin{aligned} -\mathscr{Z}_r \dot{U}^T - \mathscr{C}_i {\sigma_1}^i &= \mathscr{C}_1 {\sigma_1}^1 + \mathscr{C}_2 {\sigma_1}^2 + \mathscr{C}_3 {\sigma_1}^3 \\ -\mathfrak{D}_1 {\sigma_1}^i &= \mathfrak{D}_1 {\sigma_1}^1 + \mathfrak{D}_2 {\sigma_1}^2 + \mathfrak{D}_3 {\sigma_1}^3 \\ -\dot{U}^T + \mathfrak{H}_i {\sigma_1}^i &= \mathfrak{H}_1 {\sigma_1}^1 + \mathfrak{H}_2 {\sigma_1}^2 + \mathfrak{H}_3 {\sigma_1}^3 \\ \mathscr{M}_i \dot{\sigma}_1{}^i + \mathscr{M}_1 \dot{\sigma}_1{}^1 + \mathscr{M}_2 \dot{\sigma}_1{}^2 + \mathscr{M}_3 \dot{\sigma}_1{}^3 &= W_r(-\mathscr{N}_i {\sigma_1}^i + \mathscr{N}_1 {\sigma_1}^1 + \mathscr{N}_2 {\sigma_1}^2 + \mathscr{N}_3 {\sigma_1}^3), \end{aligned} \tag{41}$$

where W_r is warp stiffness associated with the buffer and $\mathscr{Z}_r$ is the buffer impedance such that $\sigma^T = -\mathscr{Z}_r \dot{U}^T$. From the first three of equations (41), one finds that

$$\begin{aligned} {\sigma_1}^2 &= \frac{{\sigma_1}^i(S_{3r}\mathfrak{D}_i - S_{ir}^*\mathfrak{D}_3) + {\sigma_1}^1(S_{3r}\mathfrak{D}_1 - S_{1r}\mathfrak{D}_3)}{S_{2r}\mathfrak{D}_3 - S_{3r}\mathfrak{D}_2}, \\ {\sigma_1}^2 &= \frac{{\sigma_1}^i(S_{2r}\mathfrak{D}_i - S_{ir}^*\mathfrak{D}_2) + {\sigma_1}^1(S_{2r}\mathfrak{D}_1 - S_{1r}\mathfrak{D}_2)}{S_{3r}\mathfrak{D}_2 - S_{2r}\mathfrak{D}_3}, \\ S_{ir}^* &= S_{ir} - 2\mathfrak{H}_i \end{aligned} \tag{42}$$

and S_{jr} is defined by replacing l by r in (31). From (42) and the last of equations (41), it follows that

$$a_r \dot{\sigma}_1{}^1 + b_r {\sigma_1}^1 = d_{ri} \dot{\sigma}_1{}^i + e_r {\sigma_1}^i \tag{43}$$

where a_r and b_r are defined by (33), and

$$\begin{aligned} d_{ri} &= -\delta_{i1} a_r + 2\mathfrak{H}_i(\mathfrak{D}_2 \mathscr{M}_3 - \mathfrak{D}_3 \mathscr{M}_2) \\ e_{ri} &= W_r \cos\theta[(S_{3r}\mathfrak{D}_2 - S_{2r}\mathfrak{D}_3)\mathscr{N}_i + (S_{3r}\mathfrak{D}_i - S_{ir}^*\mathfrak{D}_3)\mathscr{N}_2 + (S_{ir}^*\mathfrak{D}_2 - S_{2r}\mathfrak{D}_i)\mathscr{N}_3] \ . \end{aligned} \tag{44}$$

The expression for ${\sigma_1}^i$ to be used at $x = L$ may be obtained directly from (37) by using the retarded time $t - t_i$ instead of t, where t_i is the time required for the incident ith wave to traverse the composite; i.e.

$$t_i = H/V_i, \tag{45}$$

and V_i is the velocity of the wave. Using (37) and the integrating factor $\exp(tb_r/a_r)$ to integrate equation (43) from t_i to t, one finds that, for $t > t_i$,

$${\sigma_1}^1 = {\sigma_1}^1(t = t_i)\exp\left[\frac{b_r}{a_r}(t_i - t)\right] + \frac{e_{ri}\gamma_i}{b_r}\left\{1 - \exp\left[\frac{b_r}{a_r}(t_i - t)\right]\right\} + \frac{\delta_i}{a_r}\left(e_{ri} - b_l\frac{d_{ri}}{a_l}\right)K,$$

$$K = \begin{cases} \dfrac{\exp\left[\dfrac{b_l}{a_l}(t_i - t)\right] - \exp\left[\dfrac{b_r}{a_r}(t_i - t)\right]}{\left(\dfrac{b_r}{a_r} - \dfrac{b_l}{a_l}\right)}, & \text{if } \dfrac{b_r}{a_r} \neq \dfrac{b_l}{a_l} \\ (t - t_i)\exp\left(\dfrac{b_l t_i}{a_l} - \dfrac{b_r t}{a_r}\right), & \text{if } \dfrac{b_r}{a_r} = \dfrac{b_l}{a_l}. \end{cases} \tag{46}$$

As was done for equation (34), one now evaluates ${\sigma_1}^1(t = t_i)$ by imposing conditions at the initial time of the interaction $t = t_i$ and by using equation (15). Although equation (15) requires the use of total stresses and displacements, the following argument will show that,

at the onset of each of the interactions [1, 2 and 3], the individual modes can be used in (15). At the onset of interaction [3] in Fig. 6, $t = t_3$, the total stresses and displacements are equal to those of interaction [3]. For time $t_3 \leq t \leq t_2$, only the terms relating to interaction [3] appear in the boundary conditions at $x = H$, including equation (15), which may be rewritten as

$$\sigma_1 - \sigma_2 = -W_r(u_1 - u_2). \tag{15}$$

At $t = t_2$, when the second wave arrives, the contributions from interactions [2 and 3] will now appear in the boundary conditions. However, since up to this time the continuous quantities from interaction [3] have satisfied (15) and since at $t = t_2$ the sum must satisfy (15), then it follows that, at $t = t_2$, interaction [2] quantities must satisfy (15) independently of those from interaction [3]. By pursuing the argument farther, one can see that, at $t = t_1$, interaction [1] quantities must satisfy (15) independently of the continuous quantities from the previous interactions. By these arguments, one finds that (15) will be satisfied by requiring that, at $x = H$, $t = t_i$,

$$[\sigma_1 - \sigma_2]_i = -W_r[u_1 - u_2]_i, \tag{47}$$

where in this equation [ ] represents the jump in the quantity. However, at $t = t_i$, the contribution to the displacements from the ith interaction is zero, and, therefore, $[u_1 - u_2]_i = 0$. Consequently, the left side of (47) is also zero and leads to

$$(\mathscr{M}_i \sigma_1{}^i + \mathscr{M}_1 \sigma_1{}^1 + \mathscr{M}_2 \sigma_1{}^2 + \mathscr{M}_3 \sigma_1{}^3) \Big|_{t=t_i} = 0. \tag{48}$$

By substituting (42) into (48) and solving for $\sigma_1{}^1(t = t_i)$, one finds that

$$\sigma_1{}^1(t = t_i) = \frac{d_{ri}}{a_r} \sigma_1{}^i(0). \tag{49}$$

To complete the solution, equations (46 and 49) are evaluated at $x = H$ for each of the three interactions. These results are substituted into (42) and the first of (41) to evaluate $\dot{U}^T$ for each of the three transmitted longitudinal waves.

DISCUSSION OF RESULTS

In the analysis of composite materials, one is interested in both the static and dynamic response to applied loads. For the determination of this response, the theoretical analysis of the previous sections has resulted in a partial determination of the gross static elastic constants and the wave propagation characteristics. Calculations based on these analyses will, in the second part of this paper, be compared to experiment; however, for the present, to illustrate the nature of these results, a few calculations on a laminated composite composed of alternating layers of polymethyl methacrylate (PMMA) and aluminum will be presented. Specific properties of the composite are given in Table 1.

Table 1. Composite properties

Constituent	Lamé constants (g/cm-μ sec^2) λ	μ	Mass density (g/cm^3) ρ	Thickness (cm) d
Aluminum	0·569	0·272	2·7	0·0813
PMMA	0·0412	0·0229	1·2	0·0762

The analysis of the static compression test results in equation (25) which represents the average static longitudinal stiffness of the composite for $\theta = 0$. This quantity is related to the average Young's modulus, E, by

$$F = E(1 - \nu)/[(1 + \nu)(1 - 2\nu)].$$

If the specimen in this experiment had been deformed in one-dimensional stress instead of one-dimensional strain, then equation (25) would be a measure of the average Young's modulus of the composite.

The behavior predicted by equation (25) for the static compression test is shown in Fig. 7 for PMMA buffer plates and also for aluminum buffer plates. In this figure, the ordinate is normalized to the stiffness F_∞ of an infinitely thick specimen, i.e. for $L \to \infty$

$$F \to F_\infty = \frac{\mathfrak{G}_1\mathfrak{E}_2 - \mathfrak{G}_2\mathfrak{E}_1}{\mathfrak{G}_1\mathfrak{F}_2 - \mathfrak{G}_2\mathfrak{F}_1}.$$

The abscissa is normalized to the unit cell dimension $h = d_1 + d_2$.

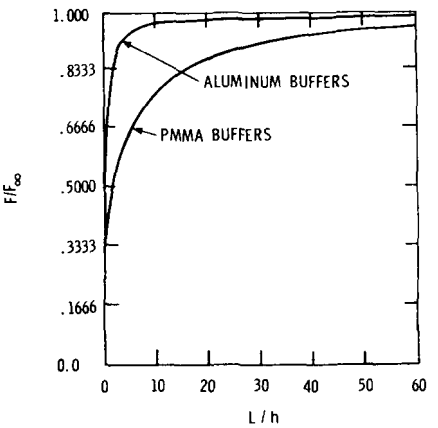

Fig. 7. The static compression experiment with PMMA and aluminum buffers.

The difference in these two curves occurs because the W for the aluminum buffers is approximately ten times that of the PMMA buffers. It is important to note that F_∞ is equal to the stiffness of an internally bonded composite. This means that, for sufficiently thick composites, the stiffness is not affected by the internal bonds; however, thinner specimens will exhibit significant differences which depend not only on the composite thickness but on the properties of the buffers. For example the debonded composite will exhibit only 80 per cent of the bonded stiffness when it is 30 unit cells thick ($L/h = 15$) and compressed between PMMA buffers.

In accordance with the discussion of Saint Venant's principle given in the Introduction, one should question the results of the present theory for small values of L/h. One cannot categorically assign a minimum value to the L/h based on theory, but, in view of Fig. 7 one can state that this minimum value will depend on the value of W. As the stiffness of the buffer plates increases, W increases and the interface warping becomes less significant, thus reducing the minimum value of L/h.

The behavior of the composite to transient loading conditions was examined through the analysis of the flyer-plate experiment. The analysis predicts the particle velocity–time history of a stress wave after it has propagated through the composite and into a homogeneous buffer material. Using again the PMMA-aluminum composite with a thickness H of 0·776 cm and $\theta = 0$, one now computes the response when a thick aluminum flyer-plate strikes the composite at 0·00142 cm/μsec. The profile of the transmitted wave is plotted in Fig. 8 just after it has entered the aluminum buffer. Because $\theta = 0$, only two waves are generated in the buffer. Geometric dispersion has also been neglected in these calculations, and consequently the characteristic spreading of shock fronts which is observed in composite materials is not present in these calculations.

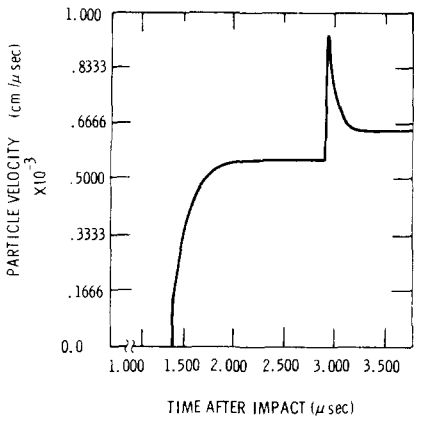

Fig. 8. The flyer-plate experiment.

The figure shows that each of the transmitted waves is composed of a shock front followed by an exponential rise or decay. The slower wave has a spike, and one would expect that this spike would be heavily attenuated if geometric dispersion were included in the calculations. Also, since as in the static case the calculations are based on the existence of a state of "quasi-equilibrium," in the time intervals where rapid changes occur the results should be viewed with some reservations. It seems reasonable to expect that these time intervals be bounded by some characteristic time associated with the wave speeds of the problem and the thicknesses of the composite layers.

The theory predicts that during the early part of the experiment, the composite constituents slide relative to each other, but, eventually, they all move at the same velocity. The final amplitude of the stress wave approaches the amplitude which would exist if the composite had remained bonded throughout the experiment.

In Part II of this paper, this theory will be compared with experiment to show that the concept of the warping stiffness provides an accurate and highly useful tool for predicting the behavior of composite materials.

REFERENCES

1. J. C. Peck and G. A. Gurtman, Dispersive Pulse Propagation Parallel to the Interfaces of a Laminated Composite, *J. Appl. Mech.* **36**, 479–484 (1969).
2. C. D. Lundergan and D. S. Drumheller, Dispersion of Shock Waves in Composite Materials, *Shock Waves and the Mechanical Properties of Solids*, edited by J. J. Burke and V. Weiss. Syracuse University Press (1971).

3. S. Timoshenko and J. N. Goodier, *Theory of Elasticity*, 2nd edition. McGraw-Hill, New York (1951).
4. O. E. Jones and F. R. Norwood, Axially Symmetric Cross-Sectional Strain and Stress Distributions in Suddenly Loaded Cylindrical Elastic Bars, *J. Appl. Mech.* **34**, 718–724 (1967).
5. C. Sve, Time–Harmonic Waves Travelling Obliquely in a Periodically Laminated Medium, *J. Appl. Mech.* **38**, 477–482 (1971).
6. D. S. Drumheller, An Effect of Debonding in Composite Materials, *J. Appl. Mech.* **40**, 1146–1147 (1973).
7. F. R. Norwood and J. Miklowitz, Diffraction of Transient Elastic Waves by a Spherical Cavity, *J. Appl. Mech.* **34**, 735–744 (1967).

Абстракт — Проведены в последных годах эксперименты одноосно усиленных материалов показывают ненормальное поведение в характеристиках распределения волн напряжения для этих материалов. Когда бы открытые концы обоих компонентов слоистих материалов ни были подвержены умеренному давлению несколько килобаров, число станционарных распространяющихся волн, образованных внутри слоистого материала, превышало на один число волн, подсчитанных на основе обыкновенных моделей слоистых материалов. Этот эффект значительно увеличал рассеяние волн и нарастание во времени в полученной экспериментально волне напряжения.

Ключ к происхождению этого необыкновенного явления совсем элементарный. жлоистый материал разъединяется внутренно. Когда теряет силу связь между усилением и основным веществом, слоистый материал достигает добавочной степени свободы, которая является результатом добавочной стационарной распространяющейся волны. Поскольку обыкновенные модели слоистых материалов не дают возможности для этого ьазъединения, они не могут считаться за возникающую в результате балку. Однако, как указано в раньшей работе, непосредственное применение теории упругости к этой задаче является результатом скоростей волн и формами типов волн для всех волн.

Решение полной задачи, заключая определение разных амплитуд волн, было заранее препятствовано недостаточной совокупностью граничных условий. Обычной методикой являлось задавать условие непрерывности напряжений и перемещений на границе между слоистым материалом и смежным однородным материалом, где были использованы объемные средние значения для слоистых материалов. Пока эти условия необходимы и достаточны для задачи связанных слоистых материалов, но недостаточны для задачи разъединенных слоистых материалов. Добавочная степень свободы в разъединенной задаче использует необходимость добавочного граничного условия. Это добавочное граничное условие является предметом этой работы.

APPENDIX A

Derivation of the warp stiffness

The derivation of the warp stiffness is effected by considering the force system shown in Fig. 3. The horizontal displacement due to these forces will be found from the stress field. To find this stress field, one appeals to the techniques of [7] to superpose the field produced by a single line load. In the r–θ coordinate system shown in Fig. 3, the stress field due to a line force at the origin (dashed arrow) is given by

$$\sigma^*_{rr}(r, \theta) = -\frac{2P}{\pi} \cdot \frac{\cos\theta}{r}, \qquad \sigma^*_{\theta\theta} = \sigma^*_{r\theta} = 0, \tag{A.1}$$

where P is the load per unit length. In the $\tilde{x}$–$\tilde{y}$ coordinate system given in the figure, this becomes†

$$\left.\begin{aligned} \sigma^*_{xx}(x, y) &= -\frac{2P}{\pi} \cdot \frac{x^3}{r^4}, \qquad \sigma^*_{yy}(x, y) = -\frac{2P}{\pi} \cdot \frac{xy^2}{r^4}, \\ \sigma^*_{yy}(x, y) &= -\frac{2P}{\pi} \cdot \frac{x^2 y}{r^4}, \qquad r^2 = x^2 + y^2. \end{aligned}\right\} \tag{A.2}$$

† The tilde will be omitted.

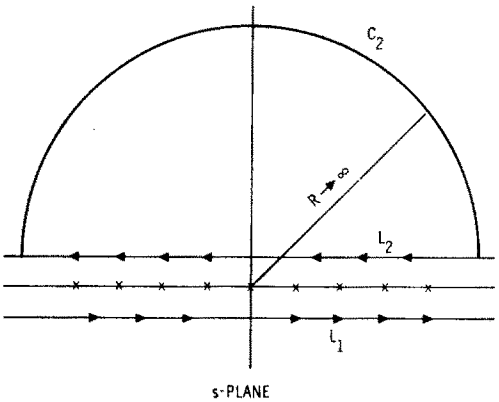

Fig. 9. Integration paths in the S-plane.

The total stress field resulting from the applied forces shown in the figure (solid arrows) is found by the application of the following lemma: Let L_1 and L_2 be oriented paths in the neighborhood of the real axis, as shown in Fig. 9. If $f(s)$ is an analytic function on and between L_1 and L_2, then

$$\sum_{n=-\infty}^{\infty} f(n) = \frac{1}{2i}\int_{L_1+L_2} \frac{f(s)e^{-i\pi s}}{\sin \pi s}\, ds.$$

The application of this lemma to the σ_{yy} stress will now be shown in detail; the results for the other stress components follow from this mutatis mutandis. The total stress is given by

$$\sigma_{yy}(x, y) = \frac{2xP}{\pi} \sum_{n=-\infty}^{\infty} e^{i\pi n} F(x, y - d + 2nd), \tag{A.4}$$

$$F(x, y) = y^2/(x^2 + y^2)^2, \qquad 4d = h/\cos\theta. \tag{A.5}$$

Therefore, one can identify

$$f(s) = e^{i\pi s} F(x, y - d + 2sd). \tag{A.6}$$

The only singularities of $f(s)$ are double poles at

$$s = \frac{d - y}{2d} + \frac{ix}{2d}, \tag{A.7}$$

so that $f(s)$ satisfies the conditions of the lemma. Hence

$$\sigma_{yy}(x, y) = \frac{2xP}{2\pi i}\int_{L_1+L_2} \frac{(y - d + 2sd)^2\, ds}{[x^2 + (y - d + 2sd)]^2 \sin \pi s}. \tag{A.8}$$

The contribution from L_2 is found by applying residue theory to the closed contour consisting of L_2 and the semicircle C_2 shown in the figure. The contribution from L_1 is found in a similar manner. The final result is

$$\sigma_{yy}(x, y) = -\frac{P}{4d^2}\,\mathfrak{Re}\,\frac{2id\sin\pi s_1 - \pi x\cos\pi s_1}{\sin^2\pi s_1}, \tag{A.9}$$

$$2ds_1 = d - y - ix. \tag{A.10}$$

The other stresses are given by

$$\sigma_{xy}(x, y) = -\frac{\pi P}{4d^2}\,\mathfrak{Im}\,\frac{\cos\pi s_1}{\sin^2\pi s_1} \tag{A.11}$$

$$\sigma_{xx}(x, y) = -\frac{P}{4d^2}\,\mathfrak{Re}\,\frac{2id\sin\pi s_1 + \pi x\cos\pi s_1}{\sin^2\pi s_1}. \tag{A.12}$$

The x displacement is found from the relation

$$e_{xx} = \frac{\partial U}{\partial x} = \frac{1+\nu}{E}\,[(1-\nu)\sigma_{xx} - \nu\sigma_{yy}]. \tag{A.13}$$

By noting that $U = 0$ at $x = \infty$, a simple integration of (A.13) leads to

$$\frac{2d}{P}\cdot\frac{E}{1+\nu}\,u = \mathfrak{Re}\left[\frac{4d(1-\nu)}{\pi}\log\tan\left(\frac{\pi s_1}{2}\right) + \frac{ix}{\sin\pi s_1}\right]. \tag{A.14}$$

Thus, at the surface, the average displacement, U, between $y = 0$ and $y = d$ is given by

$$\frac{1}{P}\frac{G}{1-\nu}\,U = \frac{2}{\pi}\int_0^1 ln\,\tan\frac{\pi}{4}(1-\xi)\,d\xi. \tag{A.15}$$

By computing the integral numerically, one finds that

$$\frac{P}{U} = 1{\cdot}207\,\frac{G}{1-\nu}. \tag{A.16}$$

The average stress between $y = 0$ and $y = d$ is $S = P/2d$. Therefore, the definition of W leads to

$$W = \frac{S}{U} = 2{\cdot}414\,\frac{G}{1-\nu}\cdot\frac{\cos\theta}{h}. \tag{A.17}$$

APPENDIX B

The solution to the field equations for a debonded composite have previously been derived by Drumheller[6] for a sinusoidal time variation. In this reference, the behavior of two adjacent laminates, $k = 1$ and 2, within the composite is represented by an appropriate set of elasticity equations whose solutions are required to satisfy the requisite periodicity

conditions. The two sets of equations are related by the boundary conditions which require that ${u_2}^{(k)}$ and ${\sigma_{22}}^{(k)}$ be continuous, and ${\sigma_{12}}^{(k)}$ be zero at the interface between the two laminates.

To solve the problem, it is assumed that the displacement potentials satisfy equations of the form

$$\phi^{(m)} = f_m(x_2)\exp[ik(n_j x_j - vt)], \qquad j = 1, 2, \tag{B.1}$$

where $n_1 = \cos\theta$, $n_2 = \sin\theta$, k is the wave number defined by 2π/wavelength, and v is the phase velocity. This reduces the problem to an algebraic system of equations whose solution for the eigenvalues and eigenfunctions leads to an eighth-order characteristic determinant.

In the small wave number limit of the solution, the eigenvalues of the characteristic determinant are determined by the following cubic equation in v^2:

$$\alpha_4 v^6 + \alpha_3 v^4 + \alpha_2 v^2 + \alpha_1 = 0 \tag{B.2}$$

where

$$\begin{aligned}
\alpha_1 &= -\theta(\rho_1/\mu_1)^3(d_1 + \theta d_2)(d_1\delta_2 + d_2\delta_1/\gamma),\\
\alpha_2 &= (\rho_1/\mu_1)^2\{n_2^2\delta_1\delta_2\theta h^2 + n_1^2(d_1 + \theta d_2)\\
&\qquad [d_1(\theta\delta_1\delta_2 + 4\delta_2\gamma - 4\gamma) + d_2(\delta_1\delta_2 - 4\theta/\gamma(1 - \delta_1))]\},\\
\alpha_3 &= -4n_1^2\mu_1/\rho_1\{[n_2^2 h^2(\theta\delta_2(\delta_1 - 1) + \gamma\delta_1(\delta_2 - 1))]\\
&\qquad + n_1^2(d_1 + \theta d_2)[d_1\gamma\delta_1(\delta_2 - 1) + d_2\delta_2(\delta_1 - 1)]\},\\
\alpha_4 &= 16{n_1}^4{n_2}^2h^2\gamma(\delta_2 - 1)(\delta_1 - 1),\\
\theta &= \rho_2/\rho_1,\\
\gamma &= \mu_2/\mu_1,
\end{aligned} \tag{B.3}$$

and

$$\delta_i = (\lambda_i + 2\mu_i)/\mu_i.$$

In general three unique values of the phase velocity, v_m, will be obtained from (B.2); however, when $n_2(n_1)$ equals zero, i.e. $\theta = 0°$ (90°), $\alpha_4 = 0(\alpha_4 = \alpha_3 = 0)$, only two (one) values of v_m are obtained. For either of these two directions, the shearing stiffness of the composite is zero and the number of propagation modes correspondingly decreases by one. In addition when $\theta = 90°$ a longitudinal distortion cannot produce sliding between the laminae so that another mode of propagation is lost.

As with all problems of this type, the deformation profiles or eigenvectors can be determined only to within an arbitrary constant. However, there are certain ratios between the various stress, displacement, and velocity components which can be determined exactly. On selecting ${}_m\sigma_{11}{}^{(1)}$ as the denominator of these ratios, one finds that not all such ratios are useful. For example, the ratio between any of the displacements components and the stress ${}_m\sigma_{11}{}^{(1)}$ approaches zero as k approaches zero. The nonzero ratios are those which relate the particle velocities, strains, and stresses to the stress ${}_m\sigma_{11}{}^{(1)}$. These ratios are

$$\frac{{}_m{u_1}^{(i)'}}{{}_m\sigma_{11}{}^{(1)}} = -D_i/\Delta$$

$$\frac{{}_m u_2^{(i)'}}{{}_m\sigma_{11}^{(1)}} = A/\Delta$$

$$\frac{{}_m\sigma_{11}^{(2)}}{{}_m\sigma_{11}^{(1)}} = \frac{\left[-\frac{\lambda_2}{\delta_2\gamma}B - \left(\frac{\lambda_2}{\delta_2} + \mu_2\right)2n_1 D_2\right]}{\Delta} \tag{B.4}$$

$$\frac{{}_m\sigma_{22}^{(i)}}{{}_m\sigma_{11}^{(1)}} = -\mu_1 B/\Delta$$

$$\frac{{}_m\sigma_{12}^{(i)}}{{}_m\sigma_{11}^{(1)}} = 0$$

where

$$\begin{aligned}
\Delta &= -\frac{\lambda_1}{\delta_1}B_2 - \left(\frac{\lambda_1}{\delta_1} + \mu_1\right)2n_1 D_1,\\
A &= n_2 h S_2 S_1,\\
B &= -\beta^2 S_3 S_2 S_1,\\
D_i &= \beta^2 S_3 n_1(\delta_i - 2)S_2/(\delta_i\gamma),\\
\beta &= C_m{}^2\rho_1/\mu_1,\\
S_1 &= [4n_1{}^2\gamma(\delta_2 - 1) - \delta_2\theta\beta^2]/(\delta_2\gamma),\\
S_2 &= [4n_1{}^2(\delta_1 - 1) - \delta_1\beta^2]/\delta_1
\end{aligned} \tag{B.5}$$

and

$$S_3 = d_1 + \theta d_2 .$$

For right-traveling waves, the ratios involving particle velocities can be determined from (B.4) in combination with

$${}_m\dot{u}_j^{(i)} = -V_m\,{}_m u_j^{(i)'}. \tag{B.6}$$

Finally, when displacement ratios are required they are found to be equal to the ratios of the corresponding strains so that, for example, $u_1{}^{(i)}/u_2{}^{(i)}$ is equal to the first of (B.4) divided by the second of (B.4). A similar result holds for time derivatives of the stresses. In this case, for example,

$$\frac{{}_m\dot{\sigma}_{22}^{(i)}}{{}_m\dot{\sigma}_{11}^{(1)}} = \frac{{}_m\sigma_{22}^{(i)}}{{}_m\sigma_{11}^{(1)}}. \tag{B.7}$$